Check for updates

Received: 19 April 2023 | Revised: 25 July 2023 | Accepted: 31 August 2023

DOI: 10.1111/1750-3841.16768

Journal of Food Science WILEY

ORIGINAL ARTICLE

Integrated Food Science

Optimization of complex coacervation parameters for the production of encapsulated black garlic using response surface methodology

Hatice Kubra Sasmaz[1] | **Eda Adal**[2] | **Pınar Kadiroğlu**[1] | **Serkan Selli**[3] | **Turkan Uzlasir**[1] | **Hasim Kelebek**[1]

[1]Department of Food Engineering, Faculty of Engineering, Adana Alparslan Turkes Science and Technology University, Adana, Turkey

[2]Faculty of Tourism, Gastronomy and Culinary Arts, Iskenderun Technical University, Hatay, Turkey

[3]Department of Food Engineering, Faculty of Agriculture, Cukurova University, Adana, Turkey

Correspondence
Hasim Kelebek, Department of Food Engineering, Faculty of Engineering, Adana Alparslan Turkes Science and Technology University, Adana 01250, Turkey.
Email: hkelebek@atu.edu.tr

Funding information
Scientific and Technological Research Council of Türkiye (TUBITAK), Grant/Award Number: TOVAG 219O174

Abstract: The purpose of this study was to optimize black garlic encapsulation parameters (core/coating ratio, extract concentration, and coacervate/maltodextrin [MD] ratio) using central composite design of the response surface methodology based on encapsulation efficiency (EE) (%). The optimum parameters were determined as 4.0 for the coating material/core ratio, 50% for the extract concentration, and 6.0 for the MD/coacervate ratio depending on the EE (%). The antioxidant activity values were determined as 101 and 134 μmol Trolox/100 g dry weight (DW) for the 2,2-diphenyl-1-picrylhydrazyl and 2,2′-azino-bis(3-ethylbenzothiazoline-6-sulfonic acid) methods, respectively, whereas the total phenolic content was 49 mg gallic acid equivalent/100 g DW for the encapsulated black garlic samples. *S*-Allyl-L-cysteine (SAC), *γ*-L-glutamyl-SAC (GSAC), *γ*-L-glutamyl-(*S*)-*trans*-1-propenyl-L-cysteine, and allicin were the organosulfur (OS) compounds determined in the samples. The SAC concentration of the encapsulated black garlic samples was determined as 22.36 mg/g, whereas the GSAC content was found at a lower concentration (0.33 mg/g) compared to SAC. The allicin content was quantified to be 0.31 mg/g. The encapsulated samples were also characterized by scanning electron microscopy (SEM) and Fourier transform infrared (FT-IR) spectroscopy. The FT-IR analysis revealed specific functional groups, including hydroxyl, carbonyl, and glycosidic linkage. The interaction between lentil protein isolate and pectin was strong enough to encourage capsule formation as visualized in the SEM images. This study shows the potential of black garlic coacervates as a functional ingredient for the food industry due to their stability, solubility, and preservation of OS and antioxidant compounds.

KEYWORDS
black garlic, complex coacervation, encapsulation, lentil protein isolate, optimization, scanning electron microscopy

This is an open access article under the terms of the Creative Commons Attribution-NonCommercial-NoDerivs License, which permits use and distribution in any medium, provided the original work is properly cited, the use is non-commercial and no modifications or adaptations are made.
© 2023 The Authors. *Journal of Food Science* published by Wiley Periodicals LLC on behalf of Institute of Food Technologists.

1 | INTRODUCTION

Black garlic is obtained by fermenting raw (white, fresh) garlic under controlled conditions with high humidity (70%–90%) and high temperature (60–90°C) during a certain time period (Kim et al., 2013; Zhang et al., 2014). As a result of the reactions occurring during the fermentation, significant quantitative and compositional changes occur in the bioactive compounds such as sulfur compounds, phenolics, proteins, and vitamins (Kim et al., 2013). Alliin and allicin, which give garlic its distinctive smell, are converted into water-soluble antioxidant constituents, including flavonoids and alkaloids, *S*-allyl-L-cysteine (SAC), and tetrahydro-β-carbolines during the fermentation process resulting in a decrease in their amount (Corzo-Martínez et al., 2007). SAC, the main organosulfur (OS) compound in black garlic, is about six times higher (98–194 μg/g) in black garlic compared to raw garlic (20–30 μg/g) (García-Villalón et al., 2016; Zhang et al., 2014). SAC is the most important OS compound with its crucial pharmacological properties, including anti-hepatopathy, anti-carcinogenic, neurotrophic, and antioxidant activities (Park et al., 2017).

Encapsulation is a technique used for obtaining products with new, improved, and useful properties by encasing the raw materials with solid, liquid, or gaseous active substances in a polymeric matrix (Dubey et al., 2009; Jyothi et al., 2010). Its main purpose is to preserve the core material from adverse conditions, including undesirable effects of light, heat, moisture, and oxygen to extend the product's shelf life and provide a slower release of its compounds to enhance its functionality and efficacy over a longer period (Grgić et al., 2020; Shahidi & Han, 1993; Speranza et al., 2017).

Various techniques are used for encapsulation applications in food industry. The complex coacervation technique is a coalescent phase separation that generally occurs during an interaction of two or more oppositely charged polymers in an aqueous medium under proper conditions (Gouin, 2004). The separation of the liquid/liquid phase occurs spontaneously creating a polymer-rich phase in equilibrium with a polymer solution (Tylkowski et al., 2017). The first one is named as the "complex coacervate" and the second one is the "supernatant" (Eratte et al., 2014). A complex coacervate must spontaneously engulf dispersed droplets or solids to create shells to produce microcapsules. This engulfing occurs when the interface reduces the free energy, and coacervate is adsorbed on the surface of the dispersed droplets or encapsulated solid particles (Earnest et al., 2009). If the complex coacervate does not absorb such surfaces, it does not form a capsule. Hence, this complex coacervation adsorption action is the most important factor in the encapsulation processes. The biopolymer structure is critical in establishing the complex coacervates to form food-grade microcapsules. Most of the complex coacervates are formed by the interactions between a polysaccharide and a protein (Eratte et al., 2014).

Optimization is a crucial procedure to improve the efficiency of process operations and the acceptability of the process yield. The response surface method (RSM) is a statistical technique that is often used in optimization processes.

In studies conducted on black garlic, the focus has mainly been on its physicochemical properties, antioxidant capacity, and health benefits. To the best of the authors' knowledge, there has been no study in the literature about the optimization of the encapsulation conditions of black garlic and their effects on the antioxidant activity, total phenolic content (TPC), and OS compounds of the encapsulated black garlic samples. The importance of black garlic encapsulation studies lies in their approach to preserving the beneficial properties of black garlic through encapsulation techniques. The aim of encapsulating black garlic is to preserve the bioactive compounds present in black garlic intact, increase their stability, and provide controlled release mechanisms. Encapsulation of black garlic is a novel and innovative approach to exploit its potential benefits for various applications in the food, pharmaceutical, and nutraceutical industries. Thus, the goal of this work was to optimize the encapsulation parameters (core/coating [C/C] ratio, extract concentration, and coacervate/maltodextrin [MD] ratio) of black garlic. The RSM and central composite design (CCD) techniques were used based on the encapsulation yield (%). Sulfur compounds and antioxidant activity potentials (with two different methods, 2,2-diphenyl-1-picrylhydrazyl [DPPH] and 2,2′-azino-bis(3-ethylbenzothiazoline-6-sulfonic acid) [ABTS]) were determined for the encapsulated samples produced under optimum conditions. The encapsulated samples were also examined by using Fourier transform infrared spectroscopy (FT-IR), scanning electron microscopy (SEM), hygroscopicity, and solubility analyses. This is the first study in the literature in which black garlic extract (BGE) was encapsulated by a complex coacervation method, and encapsulation parameters were optimized.

2 | MATERIALS AND METHODS

2.1 | Chemicals and reagents

HPLC-grade ethanol (64-17-5), methanol (67-56-1), acetonitrile (75-05-8), formic acid (64-18-6), and Folin–Ciocalteu reagent were purchased from the Merck Company. Lentil

17503841, 2023, 11, Downloaded from https://ift.onlinelibrary.wiley.com/doi/10.1111/1750-3841.16768 by Sakarya Teknik Universitesi, Wiley Online Library on [15/01/2024]. See the Terms and Conditions (https://onlinelibrary.wiley.com/terms-and-conditions) on Wiley Online Library for rules of use; OA articles are governed by the applicable Creative Commons License

protein isolate (LPI) was provided by AGT Food and Ingreditents, Regina, SK, Canada. Pectin (PE, from citrus peel) (9000-69-5), standard chemicals, MD (dextrose equivalent of 16.5-19.0) (9050-36-6), SAC (21,593-77-1) were obtained from Sigma-Aldrich Chemical Co. Allicin (539-86-6) was purchased from LKT Laboratories, Inc. (St. Paul, MN, USA) ABTS diammonium salt (30931-67-0), potassium persulfate (7727-21-1), and DPPH (1898-66-4) were purchased from Merck Corp., Rahway, NJ, USA. Deionized water was used to prepare the mobile phases in HPLC analyses.

Standard solutions as well as sensitive solutions were prepared daily. The ABTS radical cation was prepared by the reaction of 7 mM ABTS with 2.54 mM potassium persulfate after incubation at room temperature for 12–16 h. Prior to the assay, the ABTS solution was diluted with ethanol to obtain an absorbance value of 0.70 ± 0.02 at 734 nm.

2.2 | Black garlic samples

Raw (white, fresh) garlic used as a raw material in the study was obtained from a local producer in Kastamonu province of Türkiye in July, 2021. Production parameters were selected as humidity, temperature, and time duration based on the literature on black garlic production. In our previous study, black garlic production conditions (humidity, temperature, and duration) were optimized with a three-factor rotatable CCD of the RSM using the Design Expert program (7.1-Stat-Ease). Black garlic was produced from raw garlic in that study using the parameters of 65–85°C temperature, 70%–85% humidity, and 24–50 days. It was previously determined that the optimum conditions for black garlic production were 85% humidity, 65°C temperature, and 24 days (Sasmaz et al., 2023). In the current study, black garlics produced under these optimum conditions were used.

2.3 | Preparation of black garlic extracts for encapsulation

Black garlic was extracted according to the method by Tavares and Noreña (2019) with slight modifications. An amount of 30-g black garlic was minced with 30 mL distilled water (1:1 ratio, 50%) using a blender (Waring 8011 EB SET2). The final mixture was retained in an ultrasonic water bath for 10 min and then centrifuged for 20 min at 25°C/2900 × *g*. The BGEs were filtered by using coarse cellulose filter paper (25 μm) (Pinilla et al., 2019). BGE concentrations were prepared according to Pinilla et al. (2019).

2.4 | Determination of optimum LPI/PE mass ratio for complex coacervation

Complex coacervation was applied in reference to Lan et al. (2020). Stock solutions of LPI in 1% (w/w) and PE in 1% (w/w) were prepared separately by dissolving an exact amount of powder in distilled water and then stirred for 2 h at room temperature in order to ensure that the LPI was completely dissolved by applying ultrasound (Branson Sonifier SFX250, Branson Ultrasonics, Brookfield, CT, USA) at a setting of 50% amplitude for a period of 3 min. The pH of the solutions was adjusted to 7.0 by using 0.1 N HCl or NaOH. Fixed LPI solution (1% w/w) was mixed with PE solution with different concentrations to obtain the initial LPI/PE ratios ranging from 1:1 to 4:1. The biopolymer ratios were determined based on the data from the literature (Huang et al., 2012; Tavares & Noreña, 2019). The mixtures of LPI and PE with variable ratios were investigated in terms of turbidity (%*T*) and zeta potential (mV) by changing the pH in the range of 2.0–9.0. The pH of the mixtures was adjusted using HCl and NaOH to minimize dilution effect. The zeta potential measurements of the solutions were made prior to other analyses with a Zetasizer instrument (Nano ZS, Malvern Instruments) (Anema & Kruif, 2016). The measurements were carried out using capillary cuvettes with approximately 2-mL volume. In the case of precipitation, centrifugation or sedimentation was applied. The turbidity of the samples was determined at 600 nm with a spectrophotometer (Agilent Technologies). Optimization was performed based on the values obtained with the highest turbidity and zeta potential.

2.5 | Encapsulation of black garlic extracts by a complex coacervation

Encapsulation was carried out with complex coacervation process in accordance with the optimal pH and biopolymer ratio. The extract samples were prepared using the ratios specified in Table 1a and added to the LPI solution. The solutions were then mixed at 33,603 × *g* for 2 min in a high-speed homogenizer (IKA). The samples were then subjected to an ultrasonic homogenization (Sonifier 250) for 1 min at 20 kHz, 160 W, 50% ultrasonic power. The PE solution was slowly added to the LPI–BGE mixture and stirred at 500 rpm for 30 min. The specified proportion (Table 1a) of the MD was added after the coacervation was completed to avoid interaction. The encapsulation process was completed after the pH of the solution was brought to 3.2 and phase separation was achieved by keeping the solution at 4°C for 30 min. The capsule phase was separated and poured into aluminum petri dishes (diameter:

17503841, 2023, 11, Downloaded from https://ift.onlinelibrary.wiley.com/doi/10.1111/1750-3841.16768 by ?skenderun Teknik Universitesi, Wiley Online Library on [15/01/2024]. See the Terms and Conditions (https://onlinelibrary.wiley.com/terms-and-conditions) on Wiley Online Library for rules of use; OA articles are governed by the applicable Creative Commons License

TABLE 1a Central composite design of the variables and observed responses under different experimental conditions.

Run order	Core/coating material ratio	Extract concentration (%)	Coacervate/maltodextrin ratio	Encapsulation efficiency (%)
1	1:4.68	35.00	4.00	48.28
2	1:3	35.00	4.00	37.08
3	1:4	20.00	2.00	25.14
4	1:2	20.00	6.00	41.52
5	1:2	50.00	6.00	65.40
6	1:2	20.00	2.00	16.99
7	1:3	9.77	4.00	18.41
8	1:3	35.00	4.00	37.21
9	1:3	35.00	4.00	37.08
10	1:3	35.00	4.00	36.14
11	1:3	35.00	7.36	64.01
12	1:4	50.00	6.00	74.31
13	1:4	20.00	6.00	47.00
14	1:2	50.00	2.00	45.91
15	1:3	60.23	4.00	70.14
16	1:4	50.00	2.00	57.11
17	1:3	35.00	4.00	37.80
18	1:3	35.00	4.00	34.65
19	1:3	35.00	0.64	30.66
20	1:1.32	35.00	4.00	34.04

20 cm). Before the freeze-drying procedure, the samples were stored in a freezer at −40°C. The drying process was carried out for about 48 h in a laboratory-type freeze dryer (Christ Alpha 1–4 LDPlus, Martin Christ) (Tavares & Noreña, 2019).

2.6 | Optimization of the encapsulation by complex coacervation

An experimental design with five-level three-factor RSM method was used for the optimization of the BGE encapsulation. Optimal processing conditions were determined using the CCD method. The C/C ratio (1:2–1:4) (A), extract concentration (20%–50%) (B), and coacervate/MD ratio (C/C) (1:2–1:6) (C) were used as the independent variables. The encapsulation efficiency (EE) was treated as the dependent variable and calculated according to the following equation:

$$EE(\%) = [(\text{amount of SAC encapsulated/amount of SAC at the start})] \times 100 \quad (1)$$

The EE was determined based on the amount of SAC, which is the main component of the BGE according to the method of Pinilla et al. (2019). The amount of SAC was determined by using LC–MS/MS. The encapsulation process was performed with three replications by using the determined optimum independent variable values. The optimization was experimentally verified by examining the dependent variable (EE). A total of 43 tests were performed in the extraction process based on the experimental design, 40 experiments with 2 replications, and 3 experiments under optimum conditions. Selected process variables with their ranges are given in Table 1b.

2.7 | Antioxidant capacity analyses

The antioxidant capacity was measured by two different methods as ABTS and DPPH analyses. The DPPH and ABTS scavenging activities were determined in reference to the study by Kelebek et al. (2017) as Trolox equivalents (gallic acid equivalents, GAE) in μmol Troloks/100 g of extracts.

17503841, 2023, 11, Downloaded from https://ift.onlinelibrary.wiley.com/doi/10.1111/1750-3841.16768 by Tekirdag Tekirdag Universitesi, Wiley Online Library on [15/01/2024]. See the Terms and Conditions (https://onlinelibrary.wiley.com/terms-and-conditions) on Wiley Online Library for rules of use; OA articles are governed by the applicable Creative Commons License

TABLE 1b Independent variables, with their coded and actual values used for the *optimization* process.

	Symbol	Coded levels				
Independent variables		−1.68	−1	0	1	1.68
Core/coating material ratio	*A*	1:1.32	1:2	1:3	1:4	1:4.68
Extract concentration (%)	*B*	9.77	20.0	35.0	50.0	60.23
Coacervate/maltodextrin ratio	*C*	1:0.64	1:2	1:4	1:6	1:7.36

2.8 | Total phenolic content analysis

TPCs analysis is related to the redox reaction in which phenolic compounds reduce the Folin–Ciocalteu reagent that acts as an oxidizing compound in a basic medium. The TPC is quantified by using the absorbance of the blue color created by the reduced reagent at the end of the reaction. The TPC values of the samples in the present study were quantified by using the Folin–Ciocalteu method in reference to Kim et al. (2013) and expressed as GAE in mg/100 g of extracts.

2.9 | Analysis of the organosulfur (OS) compounds

The extractions were performed using the method available by Sasmaz et al. (2022) with minor changes. The OS compounds were analyzed by using LC–DAD–ESI–MS/MS (Agilent 1260 HPLC; Agilent Technologies, Santa Clara, CA, USA) in a positive ionization mode utilized with the following parameters: drying gas of N_2 at 12 L/min, capillary temperature of 400°C, and nebulizer pressure of 45 psi of ESI/MS detection. The analyses were performed using a Phenomenex Luna reversed-phase C-18 column with the dimension of 4.6 mm × 250 mm × 5 m. Two mobile phases were employed for the analysis: solvent A, consisting of a mixture of water and formic acid in a ratio of 99:1 (v/v), and solvent B, which was prepared by combining acetonitrile and solvent A in a ratio of 60:40 (v/v). Standard curves were computed based on the commercial standards at the concentrations existing in the extracts (1–100 mg/L) with R^2 values higher than 0.99.

2.10 | Characterization of the encapsulated black garlic samples

2.10.1 | Moisture content and water activity analysis

The moisture contents (MCs) of the samples were assessed gravimetrically by oven-drying method (Memmert GmbH UN 55) at 105°C until obtaining a constant weight (AOAC, 1990). The water activity values of the samples were determined at 25°C by using a water activity meter (Aqualab 4TE, Meter, Pullman, WA, USA).

2.10.2 | Solubility

The solubility values of the samples were evaluated in reference to Tavares and Noreña (2019). An amount of 1 g of sample was added to 100 mL of distilled water and stirred for 30 min in a stirrer and then centrifuged for 10 min at 3517 × *g* at 4°C (Hettich Universal 320R, Hettich, Tuttlingen, Germany). The supernatant was put into a beaker and dehydrated at 105°C in an oven until constant weight. The solubility (%) was computed by the weight difference.

2.10.3 | Hygroscopicity

The hygroscopicity values of the samples were assessed according to Tavares and Noreña (2019). The hygroscopicity (%) was also determined by the weight difference.

2.10.4 | Particle size distributions

A particle size analyzer (Mastersizer 3000, Malvern Panalytical, Malvern, UK) was employed to evaluate the particle size distributions of the encapsulated samples. All results were calculated by taking the average of two experiments (Akdeniz et al., 2018). Average droplet sizes were assessed based on the volume mean diameter *d*43. In addition, the span values of the samples were evaluated based on the following formula:

$$\text{Span (range)} = \frac{[d(v,90) - d(v,10)]}{d(v,50)} \quad (2)$$

where $d(v,90)$, $d(v,50)$, and $d(v,10)$ are 90%, 50%, and 10% of the total volume, respectively. Namely, $[d(v,90)–d(v,10)]$ is the range, where $(v,50)$ is the average diameter.

2.10.5 | Fourier transform infrared (FT-IR) spectroscopy

The samples were analyzed at room temperature by using an FT-IR spectrometer (Perkin Elmer Inc.). The

17503841, 2023, 11, Downloaded from https://ift.onlinelibrary.wiley.com/doi/10.1111/1750-3841.16768 by Iskenderun Teknik Universitesi, Wiley Online Library on [15/01/2024]. See the Terms and Conditions (https://onlinelibrary.wiley.com/terms-and-conditions) on Wiley Online Library for rules of use; OA articles are governed by the applicable Creative Commons License

spectrums were recorded in the 450−4000 cm^{-1} range (resolution: 4 cm^{-1}, scan speed: 1 cm/s). Measurements were performed twice for each sample.

2.10.6 | Morphological analysis by scanning electron microscopy

The structure and the surface morphologies of the samples were evaluated by SEM. The samples were fixed and sputter-coated with a thin layer of gold with a coater (Q150R Plus Sputter Coater Combined System, Quorum Technologies, Lewes, UK). The photos were taken at a beam-accelerating voltage of 5 kV on an SEM system (Quanta Field Emission 650, FEI, Oregon, USA). The cross section and surface morphology images were obtained with a magnification of 20,000.

2.11 | Statistical analyses

The optimization study was carried out by applying RSM and CCD methods to find the best factor levels and obtain the best response. A three-factor (C/C ratio, extract concentration (20%–50%), and coacervate/MD ratio) and five-level design were used in the study. The analysis of variance (ANOVA) was used to determine the suitability of the experimental data and the model. Significant terms in the models were assessed by using the *F*-statistic. Based on the analysis, the insignificant factors ($p > 0.05$) were taken out of the model and then the regression coefficients were recomputed.

3 | RESULTS AND DISCUSSION

3.1 | Effect of biopolymer ratio and pH on the formation of complex coacervation

The impacts of the biopolymer ratio and pH on the formation of protein–polysaccharide complexes were examined in the study. The LPI and different ratios of PE were used in the formation of the complexes. The turbidity and the zeta potential analyses were implemented based on the biopolymer ratio in the samples. The biopolymer ratio with the closest zeta potential to 0, turbidity value, and the highest coacervation efficiency was determined as the optimum ratio for the complex formation. The total biopolymer ratio was determined as 1% (w/w). The ratios of the LPI to PE of 1:1, 2:1, and 4:1 were studied. As can be seen in Figure 1a, the pH value at which the maximum complex coacervate is formed shifted to the right as the LPI/PE ratio increased. A similar change was visible in the complex coacervation study of LPI with different gums by Aryee and Nickerson (2014). Figure 1b depicts the pH-dependent variation

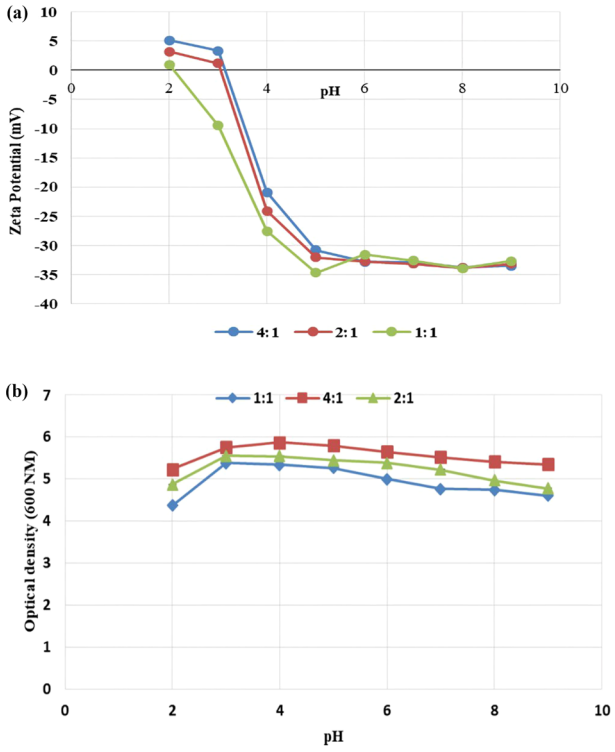

FIGURE 1 (a) pH-dependent change of the zeta potential value of the lentil protein isolate (LPI)/pectin (PE) complex formation at different biopolymer ratios. (b) Change of the turbidity value of the lentil protein isolate (LPI)/pectin (PE) complex formation as a function of pH and different biopolymer ratios.

of the biopolymer ratio change and the data show parallelism with the zeta potential and the maximum turbidity between the pH levels of 2.0 and 3.0. Similar results were observed for the ratios of 2:1 and 4:1. As the increase in the protein ratio caused aggregation among the proteins, the 2:1 ratio was chosen as the optimum ratio (Flanagan et al., 2015).

In the complexes prepared with the LPI and PE, the electrical charge had a positive value up to the isoelectric point but it changed to a negative value after this point. The zeta potential of the complexes formed with PE declined from +3.2 to −33.1 mV between the pH values of 2.0 and 9.0 and the minimum value was observed at the pH value of 3.2 (Figure 1a). This point was assessed as the pH value at which the solubility of the complex was the lowest with maximum coacervation (Anema & Kruif, 2016). These findings were also confirmed by the turbidity tests (Figure 1b).

3.2 | Optimum production conditions for the encapsulated garlic samples

A 5-level and 3-factor experimental design with 43 experiments was employed to decide the optimum encapsulation parameters affecting the responses based on the EE (%).

17503841, 2023, 11, Downloaded from https://ift.onlinelibrary.wiley.com/doi/10.1111/1750-3841.16768 by Iskenderun Teknik Universitesi, Wiley Online Library on [15/01/2024]. See the Terms and Conditions (https://onlinelibrary.wiley.com/terms-and-conditions) on Wiley Online Library for rules of use; OA articles are governed by the applicable Creative Commons License

TABLE 1c Experimental design for the encapsulation of black garlic samples.

Run order	*A*	*B*	*C*	Core/coating material ratio	Extract concentration (%)	Coacervate/ maltodextrin ratio
1	0	1.68	0	1:3	60.23	4
2	0	0	0	1:3	35	4
3	−1	1	−1	1:2	50	2
4	−1.68	0	0	1:1.32	35	4
5	0	0	0	1:3	35	4
6	0	0	1.68	1:3	35	7.36
7	0	−1.68	0	1:3	9.77	4
8	1	1	−1	1:4	50	2
9	0	0	0	1.3	35	4
10	−1	−1	−1	1:2	20	2
11	1	−1	−1	1:4	20	2
12	1	1	1	1:4	50	6
13	0	0	0	1:3	35	4
14	−1	−1	1	1:2	20	6
15	1	−1	1	1:4	20	6
16	1.68	0	0	1:4.68	35	4
17	0	0	0	1:3	35	4
18	−1	1	1	1:2	50	6
19	0	0	−1.68	1:3	35	0.64
20	0	0	0	1:3	35	4

The EE value was computed based on the amount of SAC that is the major component of the BGEs. The fermentation process converts allicin to SAC that is a bioactive substance found in black garlic (Bae et al., 2012).

The values of the independent variables were evaluated according to the highest EE from 20 products that were obtained in-line with the experimental design (Table 1c). The optimization process was performed by using the parameters shown in Table 1c. A mathematical model was created with multiple regression analysis for the dependent variable, whereas the important terms in the model were assessed by the ANOVA. Insignificant factors ($p > 0.05$) were determined and removed from the model and the coefficients of regression were computed again. The "lack of fit value" was used to assess the suitability of the model (Tables 1d and 1e). The four criteria used for this purpose were regression coefficient (R^2), adjusted regression coefficient (Adj-R^2), predicted multiple determination coefficient (Pre.-R^2), and predicted residual error sum of squares. It was assumed that the residual error values were independent of each other. To validate this assumption, residual error plots were generated against predicted values with a normal percent probability. In determining the optimum encapsulation parameters, the desirability function method was used together with the desirability tests and the response curves (Candioti et al., 2014). The effects of the factors on the response were evaluated by considering the ANOVA chart. The relationship between the factors and the response was evaluated with a numerical model by employing regression analysis and the linear terms of the factors, and the interaction effect terms were included in the models. The lack of fit (model inconsistency) and increase in the sum-of-squares were then analyzed (Table 1d). It was determined that the quadratic model was suitable (Table 1e). The ANOVA table showing the individual effects of the linear, quadratic, and interaction terms on the responses of all three factors (coating agent/core ratio, extract concentration, MD/coacervate ratio) is presented in Table 1f. The importance of the effects for the model was determined according to the *F* and *p*-values. It was aimed to make the regression model meaningful with the "lack of fit" value, which expresses the mathematical unsuitability of the model to be insignificant ($p > 0.05$). A lack of fit value of "$p > 0.10$" shows that the model was suitable for the data. The higher R^2 values ($0 > 0.90$) showed that the EE was suitable for modeling the encapsulation parameters (Table 1g). The closeness of the Pre-R^2 and Adj.-R^2 values showed that the fitted model was suitable for estimation. Residuals were important in testing these assumptions and determining the fit

17503841, 2023, 11, Downloaded from https://ift.onlinelibrary.wiley.com/doi/10.1111/1750-3841.16768 by Iskenderun Teknik Universitesi, Wiley Online Library on [15/01/2024]. See the Terms and Conditions (https://onlinelibrary.wiley.com/terms-and-conditions) on Wiley Online Library for rules of use; OA articles are governed by the applicable Creative Commons License

TABLE 1d Model inconsistency (lack of fit) test related to the encapsulation efficiency.

Source	Sum of squares	Degrees of freedom	Mean of squares	*F* Value	*p* Value
Linear	423.67	11	38.52	30.74	0.0007
2FI	403.58	8	50.45	40.26	0.0004
Quadratic	**19.17**	**5**	**3.83**	**3.06**	**0.1225**
Cubic	12.21	1	12.21	9.74	0.0262
Pure error	6.27	5	1.25		

TABLE 1e The sequential model sum of squares related to the encapsulation efficiency.

Source	Sum of squares	Degrees of freedom	Mean of squares	*F* Value	*p* Value
Average vs. total	36,883.7	1	36,883.7		
Linear vs. average	4563.9	3	1521.3	56.62	<0.0001
2FI vs. linear	20.1	3	6.7	0.21	0.8860
Quadratic vs. 2FI	**384.4**	**3**	**128.1**	**50.37**	**<0.0001**
Cubic vs. quadratic	6.9	4	1.7	0.57	0.6975
Residue	18.5	6	3.1		
Total	41,877.6	20	2093.9		

TABLE 1f Effect of linear, interaction and quadratic terms on the response of coating material/core ratio, extract concentration, maltodextrin/coacervate ratio.

Source	Sum of squares	Degrees of freedom	Mean of squares	*F* Value	*p* Value
Model	**4968.37**	**9**	**552.04**	**217.02**	**<0.0001**
A-A	243.69	1	243.69	95.80	<0.0001
B-B	2902.02	1	2902.02	1140.86	<0.0001
C-C	1418.17	1	1418.17	557.51	<0.0001
AB	5.25	1	5.25	2.06	0.1814
AC	3.08	1	3.08	1.21	0.2973
BC	11.76	1	11.76	4.62	0.0570
A^2	57.85	1	57.85	22.74	0.0008
B^2	138.93	1	138.93	54.62	<0.0001
C^2	252.61	1	252.61	99.31	<0.0001
Residue	25.44	10	2.54		
Lack of fit	19.17	5	3.83	3.06	0.1225
Pure error	6.27	5	1.25		
Total	4993.81	19			

of the model as it reflected the behavior of the random error term. The normal probability plot for the EE, the residual versus model estimate plot, and the residue versus trial sequence plot are shown in Figure 2. The quadratic model obtained for the variables that affect the EE in the optimization phase is given in Equation (3) in terms of coded variables. In addition, the relations between the values predicted from Equation (3) for the EE results and the experimental values are shown in Figure 2:

$$\begin{aligned} \mathrm{EE}\,(\%) &= 36.60 + 4.2 \times A + 14.58 \times B + 10.19 \\ &\times C + 0.81 \times A \times B - 0.62 \times A \times C - 1.21 \\ &\times B \times C + 2.00 \times A2 + 3.10 \times B2 + 4.19 \times C2 \quad (3) \end{aligned}$$

17503841, 2023, 11, Downloaded from https://ift.onlinelibrary.wiley.com/doi/10.1111/1750-3841.16768 by Tekirdag Namik Kemal Universitesi, Wiley Online Library on [15/01/2024]. See the Terms and Conditions (https://onlinelibrary.wiley.com/terms-and-conditions) on Wiley Online Library for rules of use; OA articles are governed by the applicable Creative Commons License

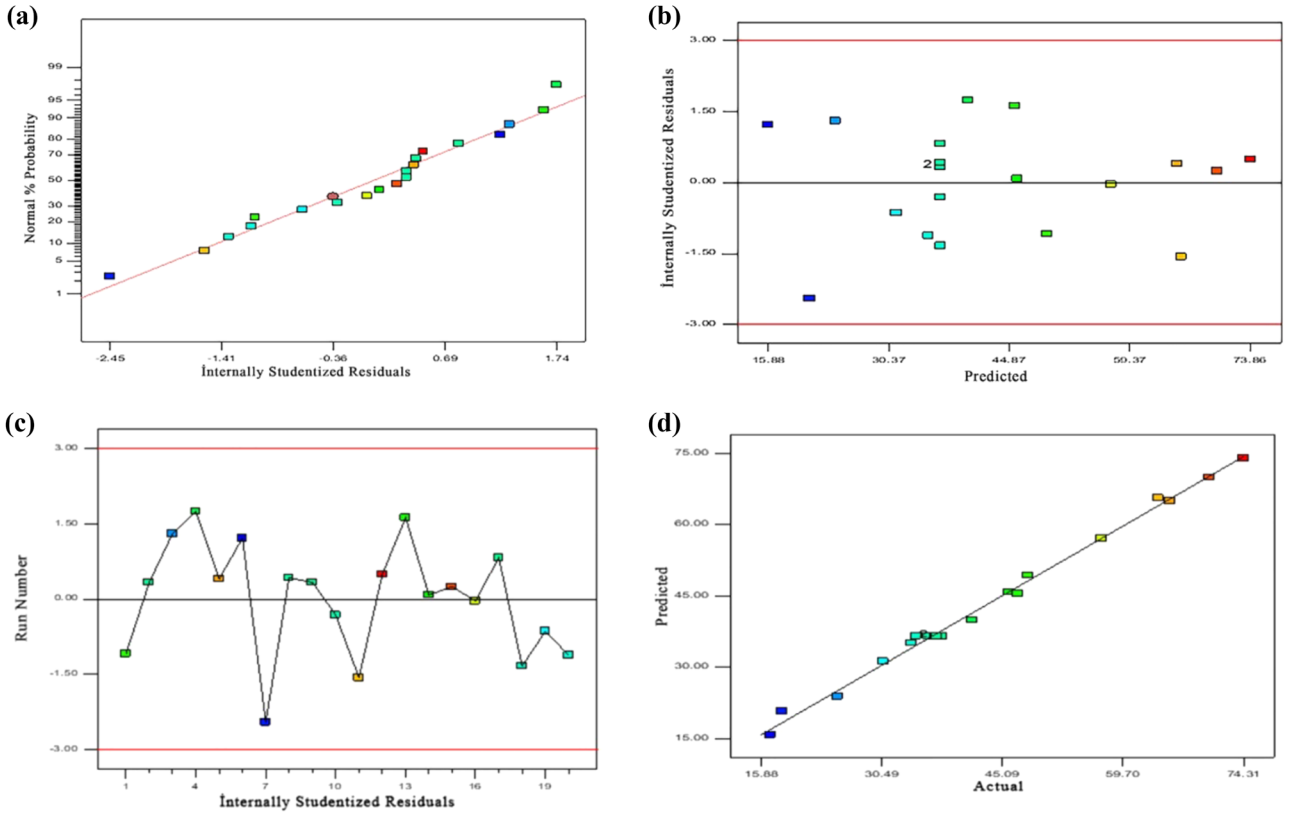

FIGURE 2 (a) Normal probability plot for the encapsulation efficiency results; (b) the graph of the residual versus model estimates; (c) the plot for the residues versus trial run numbers; (d) relationship between the predicted values and the experimental (actual) values.

TABLE 1g The terms used in the testing of the model fit.

Parameter	Value
Standard deviation	1.59
Average	42.94
R^2	0.9949
Adj.-R^2	0.9903
Pre.-R^2	0.9691
Adeq. Precision	51.414
EE. (%)	3.71
PRESS	154.08

Abbreviations: Adj.-R^2, adjusted regression coefficient; EE, encapsulation efficiency; predicted multiple determination coefficient, Pre.-R^2; PRESS, predicted residual error sum of squares.

For visual convenience, the results obtained were expressed in the form of response surface graphs and isohips curves (Figure 3). These graphs represent an infinite number of combinations of the two variables with one of the factors held constant at the center point (0) of the experimental design. The optimum conditions were determined as 4.0 for the coating material/core ratio, 50% for the extract concentration, and 6.0 for the MD/coacervate ratio based on the optimization study of the EE (Test run 12). These optimum parameters ensured the desirability condition (Table 1h). The EE was determined as 73.86% corresponding to the desirability value of 0.992 (Table 1h). The sulfur compounds, antioxidant activity, and TPC were also analyzed for the encapsulated black garlic samples produced with the obtained optimum parameters (Test run 12). Tavares and Noreña (2019) reported an EE of 51%–61% for garlic extract encapsulated by complex coacervation. In another study, Mendanha et al. (2009) encapsulated casein hydrolysate by using soy protein isolate and PE and found an EE value of 91.6%–78.8%.

3.3 | Antioxidant capacity analysis results

Antioxidants are groups of compounds that stop or slow down the oxidation reactions caused by free radicals (Kim et al., 2017). Previous research has shown that foodstuff with antioxidant activity offers an essential function for the mitigation of health problems such as cataracts, cancer, and cardiovascular problems that are believed to have resulted from oxidative stress (Huang et al., 2005). The antioxidant capacities of the black garlic samples encapsulated with the optimum parameters (Test run 12) were

17503841, 2023, 11, Downloaded from https://ift.onlinelibrary.wiley.com/doi/10.1111/1750-3841.16768 by Iskenderun Teknik Universitesi, Wiley Online Library on [15/01/2024]. See the Terms and Conditions (https://onlinelibrary.wiley.com/terms-and-conditions) on Wiley Online Library for rules of use; OA articles are governed by the applicable Creative Commons License

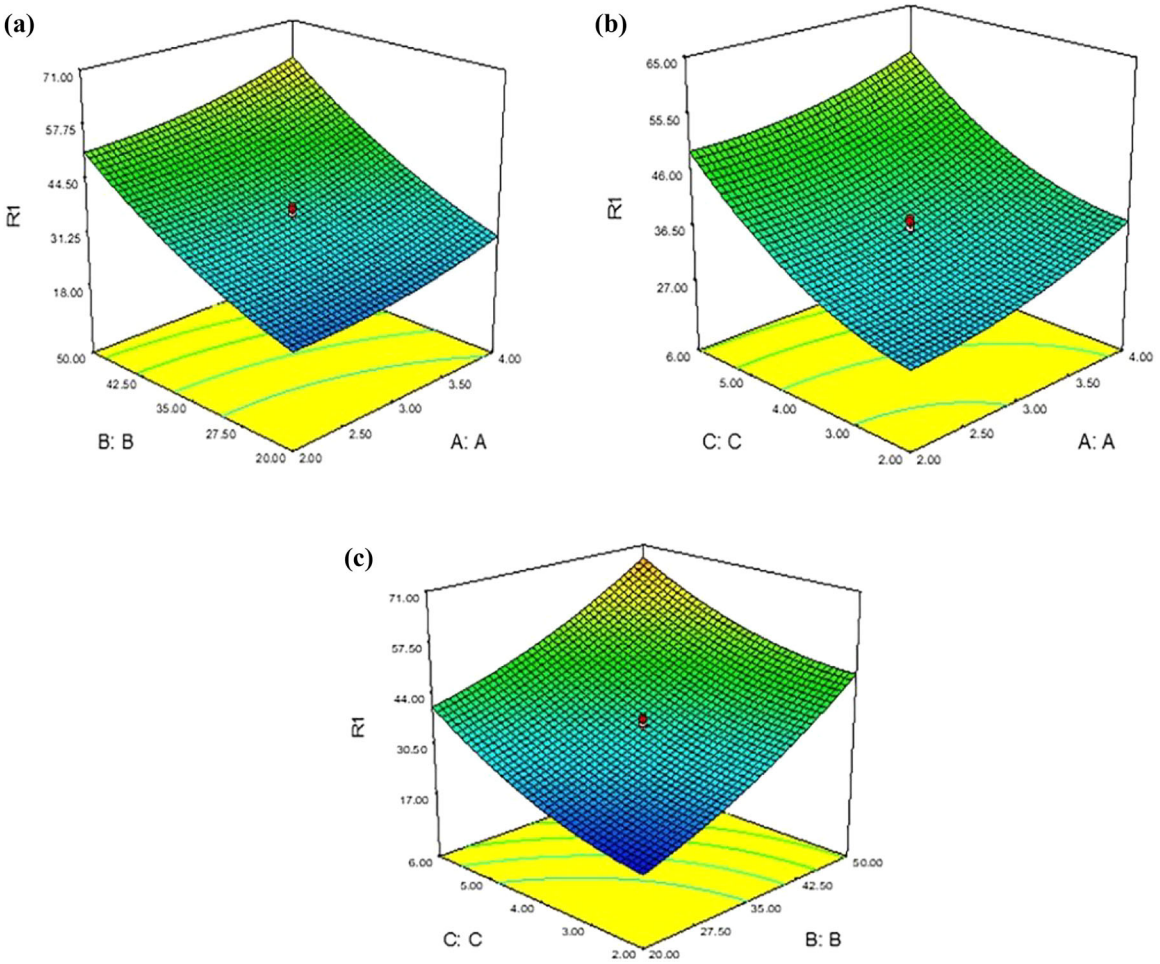

FIGURE 3 (a) The response–surface plot for the encapsulation efficiency (A: coating material/core ratio, B: extract concentration); (b) the response surface plot for the encapsulation efficiency (A: coating material/core ratio, C: maltodextine/coacervate ratio); (c) the response–surface plot for the encapsulation efficiency (B: extract concentration, C: maltodextine/coacervate ratio).

determined in the current study by two different assays (DPPH and ABTS) (Table 2a), which are the most widely used spectrophotometric methods (Sharma & Bhat, 2009). The antioxidant capacity values of the samples were determined as 101.61 μmol Trolox/100 g dry weight (DW) by the DPPH method and 134.41 μmol Trolox/100 g DW by the ABTS method (Table 2a).

3.4 | Total phenolic content (TPC) analysis results

Polyphenols are compounds that contain more than one phenol group in each molecule and constitute the most important class of natural antioxidants. The TPC values of the encapsulated black garlic produced under optimum conditions (Test run 12) are presented in Table 2a. The TPC values were determined as 49.57 mg GAE/100 g DW for these samples (Table 2a).

3.5 | Organosulfur compound analysis results

OS compounds are sulfur-containing organic molecules that are associated with the pungent odors of allium vegetables such as onions and garlic. The health benefits of garlic are due to the bioactive constituents, particularly sulfur compounds that cause bitterness. Garlics contain sulfur compounds such as alliin, allicin, and ajoene (Raghu et al., 2012).

Sulfur compounds can be grouped into two categories as water-soluble and oil-soluble compounds. Although water-soluble compounds constitute a small portion of garlic, they are thought to be the primary bioactive components for the prevention of cancer (Fukushima et al., 2001). Allium plants are recognized for producing a variety of cysteine sulfoxide complexes including alliin, propiin, and methiin (Rose et al., 2005). When the tissues of *Allium* plants are broken down, the cysteine sulfoxides react with

17503841, 2023, 11, Downloaded from https://ift.onlinelibrary.wiley.com/doi/10.1111/1750-3841.16768 by Iskenderun Teknik Universitesi, Wiley Online Library on [15/01/2024]. See the Terms and Conditions (https://onlinelibrary.wiley.com/terms-and-conditions) on Wiley Online Library for rules of use; OA articles are governed by the applicable Creative Commons License

TABLE 1h Optimum parameters determined for the encapsulation of black garlic.

Run order	Core/coating material ratio	Extract concentration (%)	Coacervate/ maltodextrin ratio	Encapsulation efficiency (%)	Desirability
1	**1:4**	**50.00**	**6.00**	**73.86**	**0.992**
2	1:3.99	50.00	6.00	73.80	0.991
3	1:4	50.00	5.98	73.72	0.990
4	1:4	49.82	6.00	73.62	0.988
5	1:3.96	50.00	6.00	73.53	0.986
6	1:4	49.71	6.00	73.47	0.985
7	1:4	48.94	6.00	72.44	0.967
8	1:3.75	50.00	6.00	71.88	0.958
9	1:3.69	50.00	6.00	71.46	0.950
10	1:3.58	50.00	6.00	70.68	0.937
11	1:4	50.00	5.46	69.68	0.919
12	1:4	50.00	5.29	68.46	0.898
13	1:2.72	50.00	6.00	66.36	0.861
14	1:2.64	50.00	6.00	66.12	0.857
15	1:2.61	50.00	5.96	65.71	0.850
16	1:2.32	50.00	6.00	65.36	0.844
17	1:3.98	50.00	4.77	64.99	0.837
18	1:2	50.00	5.76	62.97	0.802
19	1:4	50.00	2.34	57.27	0.703
20	1:2	50.00	4.54	54.14	0.648
21	1:4	29.54	6.00	51.83	0.608

TABLE 2 a Total phenolic content (TPC) and antioxidant activity (2,2-diphenyl-1-picrylhydrazyl [DPPH] and 2,2′-azino-bis(3-ethylbenzothiazoline-6-sulfonic acid) [ABTS]) values of the encapsulated black garlic samples.

Analysis	Values
TPC (mg GAE/100 g DW)	49.57 ± 0.42
DPPH (μmol Trolox/100 g DW)	101.61 ± 5.69
ABTS (μmol Trolox/100 g DW)	134.41 ± 6.46

Note: ABTS and DPPH: antioxidant capacity.
Abbreviations: DW, dry weight; GAE, gallic acid equivalent.

an enzyme called alliinase to form thiosulfinates such as allicin (Ellmore & Feldberg, 1994). Allicin's primary metabolic products are diallyl sulfides, diallyl di-sulfides, diallyl tri–tetra-sulfides, and sulfur dioxides (Das et al., 2012). SAC is an essential bioactive compound with a significant pharmacological effect in black garlic (Bae et al., 2012). It is an odorless, stable, water-soluble compound with a high antioxidant capacity. In the present study, the SAC concentration of the encapsulated black garlic was found to be 22.36 mg/g, whereas the γ-L-glutamyl-SAC (GSAC) content was 0.33 mg/g, the γ-L-glutamyl-(*S*)-*trans*-1-propenyl-L-cysteine content was 1.20 mg/g and the allicin content was 0.31 mg/g (Table 2b).

3.6 | Characterization of the encapsulated black garlic samples

3.6.1 | Moisture content, water activity, hygroscopicity, and solubility results

MC and water activity (aw) are important factors in food technology and safety due to their effect on microbial growth, lipid peroxidation, and enzymatic- and nonenzymatic reactions in foods (Kuck & Noreña, 2016). MC, water activity, and hygroscopicity parameters play crucial roles in ensuring the stability, quality, and proper storage of the powder. Additionally, the solubility and dissolution characteristics of the powder are vital considerations for its industrial application. The ability of the powder to dissolve and disperse in a solvent or medium impacts its functionality and effectiveness in various processes such as formulation development, food production, or pharmaceutical manufacturing (Tavares & Noreña, 2019, 2020).

In the present study, the mean MC of the encapsulated black garlic samples was determined as 4.68% ± 0.41% with a mean aw value of 0.42 ± 0.03. Tavares and Noreña (2019) determined the MC and water activity of powders containing microencapsulated garlic extract as 5.66%–5.69%

17503841, 2023, 11, Downloaded from https://ift.onlinelibrary.wiley.com/doi/10.1111/1750-3841.16768 by Iskenderun Teknik Universitesi, Wiley Online Library on [15/01/2024]. See the Terms and Conditions (https://onlinelibrary.wiley.com/terms-and-conditions) on Wiley Online Library for rules of use; OA articles are governed by the applicable Creative Commons License

TABLE 2 b Organosulfur compounds determined in the encapsulated black garlic samples.

Organosulfur compounds	Rt (min)	$[M-H]^+$ (m/z)	MS^2 (m/z)	Concentration (mg/g DW)
(+)-*S*-allyl-L-cysteine (SAC)	11.0	162.1	145.1, 73.1	22.36 ± 0.81
(+)-*S*-(2-propenyl)-L-cysteine sulfoxide (Isoalliin)	8.7	178.2	88.0, 160.1	Nd
γ-L-Glutamyl-*S*-allyl-L-cysteine (GSAC)	18.1	291.2	162.2, 144.8	0.33 ± 0.01
γ-L-Glutamyl-(S)-*trans*-1-propenyl-L-cysteine (GSPC)	21.5	291.2	201.1	1.20 ± 0.05
Allicin	55.3	163.2	73.2, 41.1	0.31 ± 0.01
Total				**24.20 ± 0.88**

Abbreviations: Nd: not detected; Rt: retention time.

and 0.181–0.182, respectively. In the present study, the samples were considered microbiologically stable as there is no probability of microbic development below an "aw" value of 0.60 (Rahman, 2009). The MC is an essential parameter affecting the stability of the encapsulated products. Vidović et al. (2014) reported that if the MC of food powders is less than <5%, its properties are stable. The capability of a powder sample to absorb water from the surrounding environment is known as hygroscopicity (Jaya & Das, 2004). The hygroscopic behavior of the encapsulated products is critical for food technology in terms of obtaining products with stable properties that can withstand adverse storage conditions (Šeregelj et al., 2020). In the current study, the mean hygroscopicity value of the encapsulated black garlic samples was determined as 8.14% ± 0.39%.

In the food industry, powders need to be well soluble in water to expand the variety of applications (Rocha-Selmi et al., 2013). The water solubility of the encapsulated black garlic samples in the current study was determined as 78.25% ± 1.50%. The findings of the present study are consistent with the literature. Tavares and Noreña (2019) determined the solubility of powders with microencapsulated garlic extract as 76.4%–94.3%.

3.6.2 | Particle size distributions results

Particle size analysis is widely used to characterize the size variations of the encapsulates in food formulations (Tadros et al., 2004). In the current study, the particle size of the encapsulated black garlic samples was found as 35.3 ± 0.43 μm and the span value was 2.93 ± 0.21. The low span value means a more uniform distribution (de Barros Fernandes et al., 2014). As seen in Figure 4, the distribution was not homogeneous as the samples had more than one peak in the particle size graph. This may be due to the aggregation in the samples as a result of the applied freeze drying (Yu & Lv, 2019).

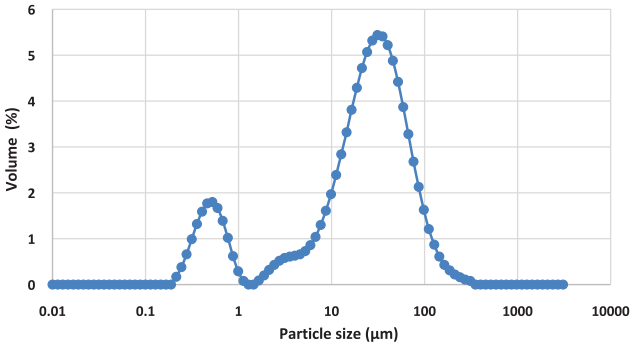

FIGURE 4 Particle size distribution of the encapsulated black garlic samples.

3.6.3 | Structural and morphological analysis results

SEM is a surface imaging device that provides important data about the visual appearance and particle size of a sample (Falsafi et al., 2020). Concave elliptical walls were observed in the SEM images of the encapsulated black garlic samples in the present study (Figure 5). Also, no apparent cracks or slits were observed on the surface of the sample indicating that the interaction between the LPI and PE was good enough to promote encapsulation formation (Tavares & Noreña, 2019). Sasmaz et al. (2023) examined the SEM images of a black garlic sample without encapsulation in their study. When the images of the black garlic samples with encapsulation in the current study and without encapsulation reported in Sasmaz et al. (2023) were compared, it was seen that the smooth and

17503841, 2023, 11, Downloaded from https://ift.onlinelibrary.wiley.com/doi/10.1111/1750-3841.16768 by Iskenderun Teknik Universitesi, Wiley Online Library on [15/01/2024]. See the Terms and Conditions (https://onlinelibrary.wiley.com/terms-and-conditions) on Wiley Online Library for rules of use; OA articles are governed by the applicable Creative Commons License

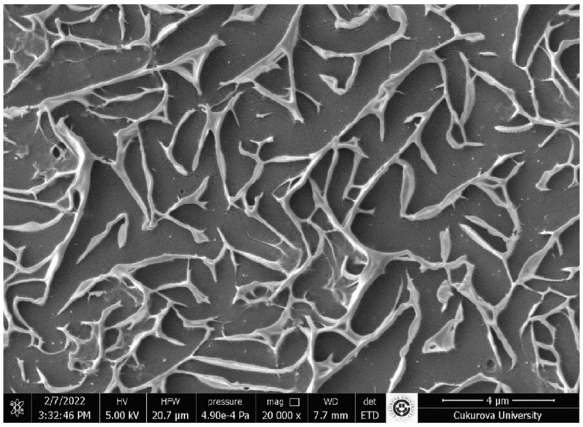

FIGURE 5 The scanning electron microscopy (SEM) image of an encapsulated black garlic sample (magnified by 20,000).

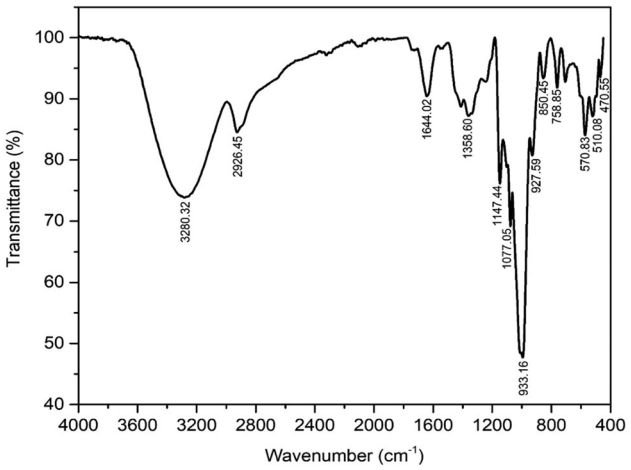

FIGURE 6 A typical mid-infrared spectrum of the encapsulated black garlic samples.

surface-covering structure was modified in the encapsulated black garlic sample (Figure 5).

3.6.4 | Fourier transform infrared (FT-IR) spectroscopy results

FT-IR analysis is one of the essential tools for the quick and effective examination of the molecules in the encapsulated chemicals in foodstuffs (Kumari et al., 2010). FT-IR data obtained in the range of 4000–400 cm^{-1} for the encapsulated black garlic sample in the present study is depicted in Figure 6. The FT-IR spectrum showed characteristic peaks near 3280 cm^{-1} (O–H stretching vibration), 2926 cm^{-1} (C–H stretching), 1644 cm^{-1} (C=O stretching), 1440–1200 cm^{-1} (carboxyl group stretching), 1200–1000 cm^{-1} (C–O–C glycosidic linkage, C–O–H, and C–O stretching vibrations) and 470 cm^{-1} (S–S stretching vibration, sulfur compounds) (Chen et al., 2015; Choi et al., 2021; Tavares & Noreña, 2020; Tavares et al., 2021). Specific functional groups such as carbonyl, hydroxyl, and glycosidic linkages were determined in the samples. These findings were similar to the observations reported by Tavares et al. (2021).

4 | CONCLUSIONS

In this study, the CCD of the RSM was used to determine the optimum values of three black garlic encapsulation parameters (kernel/coating ratio, extract concentration, and coacervate/MD ratio) based on EE (%). The optimal coating material/core ratio was determined to be 4.0, the extract concentration as 50%, and the MD/coacervate ratio as 6.0. The mean SAC and GSAC contents of the encapsulated black garlic were found as 22.36 and 0.33 mg/g, respectively, whereas the allicin content was quantified as 0.31 mg/g. It was observed that the complex coacervation with the polymeric pairs of LPI and PE was able to maintain the OS and antioxidant compounds of the black garlic samples. The resulting black garlic coacervates exhibited microbiological stability and good solubility in water which makes them suitable for various applications in the food industry.

Overall, this research demonstrated the potential of black garlic coacervates as a functional ingredient for the food industry thanks to their stability, solubility, and preservation of OS and antioxidant compounds. The black garlic coacervate powders obtained from this study can be used to fortify food products such as dairy items, bread, and cereal products. The encapsulated black garlic can act as a carrier for functional components, providing essential nutrients and potentially offering health benefits to mitigate health disorders.

AUTHOR CONTRIBUTIONS

Hatice Kubra Sasmaz: Conceptualization; Investigation; Methodology; Validation; Writing—review and editing; Formal analysis. **Eda Adal**: Conceptualization; Investigation; Methodology; Validation; Formal analysis; Funding acquisition. **Pinar Kadiroglu**: Conceptualization; Funding acquisition; Investigation; Writing —original draft; Validation; Methodology. **Serkan Selli**: Conceptualization; Investigation; Validation; Visualization; Software; Formal analysis; Methodology. **Turkan Uzlasir**: Methodology; Validation; Formal analysis; Writing —original draft. **Hasim Kelebek**: Conceptualization; Investigation; Funding acquisition; Writing—original draft; Methodology; Validation; Visualization; Writing—review and editing; Formal analysis; Data curation; Supervision.

17503841, 2023, 11, Downloaded from https://ift.onlinelibrary.wiley.com/doi/10.1111/1750-3841.16768 by Sakenderun Teknik Universitesi, Wiley Online Library on [15/01/2024]. See the Terms and Conditions (https://onlinelibrary.wiley.com/terms-and-conditions) on Wiley Online Library for rules of use; OA articles are governed by the applicable Creative Commons License

ACKNOWLEDGMENTS

This research study was financially supported by the Scientific and Technological Research Council of Türkiye (TUBITAK) (Project number: TOVAG 219O174).

CONFLICT OF INTEREST STATEMENT

The authors declare that they have no known competing financial interests or personal relationships to influence the work reported in this paper.

ORCID

Hatice Kubra Sasmaz https://orcid.org/0000-0003-4728-3151
Serkan Selli https://orcid.org/0000-0003-0450-2668
Turkan Uzlasir https://orcid.org/0000-0002-8535-2835
Hasim Kelebek https://orcid.org/0000-0002-8419-3019

REFERENCES

Akdeniz, B., Sumnu, G., & Sahin, S. (2018). Microencapsulation of phenolic compounds extracted from onion (*Allium cepa*) skin. *Journal of Food Processing and Preservation*, *42*(7), e13648. https://doi.org/10.1111/jfpp.13648

Anema, S. G., & (Kees) De Kruif, C. G. (2016). Phase separation and composition of coacervates of lactoferrin and caseins. *Food Hydrocolloids*, *52*, 670–677. https://doi.org/10.1016/j.foodhyd.2015.08.011

AOAC. (1990). *Official methods of analysis*. Association of Official Analytical Chemists (AOAC).

Aryee, F. N. A., & Nickerson, M. T. (2014). Effect of pH, biopolymer mixing ratio and salts on the formation and stability of electrostatic complexes formed within mixtures of lentil protein isolate and anionic polysaccharides (κ-carrageenan and gellan gum). *International Journal of Food Science and Technology*, *49*(1), 65–71. https://doi.org/10.1111/ijfs.12275

Bae, S. E., Cho, S. Y., Won, Y. D., Lee, S. H. A., & Park, H. J. (2012). A comparative study of the different analytical methods for analysis of *S*-allyl cysteine in black garlic by HPLC. *LWT—Food Science and Technology*, *46*(2), 532–535. https://doi.org/10.1016/j.lwt.2011.11.013

Chen, Z., Shi, J., Yang, X., Nan, B., Liu, Y., & Wang, Z. (2015). Chemical and physical characteristics and antioxidant activities of the exopolysaccharide produced by Tibetan kefir grains during milk fermentation. *International Dairy Journal*, *43*, 15–21. https://doi.org/10.1016/j.idairyj.2014.10.004

Choi, I. S., Ko, S. H., Lee, M. E., Kim, H. M., Yang, J. E., Jeong, S.-G., Lee, K. H., Chang, J. Y., Kim, J.-C., & Park, H. W. (2021). Production, characterization, and antioxidant activities of an exopolysaccharide extracted from spent media wastewater after *Leuconostoc mesenteroides* WiKim32 fermentation. *ACS Omega*, *6*(12), 8171–8178. https://doi.org/10.1021/acsomega.0c06095

Corzo-Martínez, M., Corzo, N., & Villamiel, M. (2007). Biological properties of onions and garlic. *Trends in Food Science & Technology*, *18*, 609–625. https://doi.org/10.1016/j.tifs.2007.07.011

Das, I., Acharya, A., & Saha, T. (2012). Protective effect of garlic in skin cancer. In V. R. Preedy, (Ed.), *Handbook of diet, nutrition and the skin* (pp. 300–317). Wageningen Academic Publishers.

de Barros Fernandes, R. V., Borges, S. V., & Botrel, D. A. (2014). Gum arabic/starch/maltodextrin/inulin as wall materials on the microencapsulation of rosemary essential oil. *Carbohydrate Polymers*, *101*, 524–532. https://doi.org/10.1016/j.carbpol.2013.09.083

Dubey, R., Shami, T. C., & Bhasker, R. K. U. (2009). Microencapsulation technology and applications. *Defense Science Journal*, *59*(1), 82–95.

Earnest, C. P., Hammar, M. K., Munsey, M., Mikus, C. R., David, R. M., Bralley, J. A., & Church, T. S. (2009). Microencapsulated foods as a functional delivery vehicle for omega-3 fatty acids: A pilot study. *Journal of the International Society of Sports Nutrition*, *6*, 12–18. https://doi.org/10.1186/1550-2783-6-12

Ellmore, G. S., & Feldberg, R. S. (1994). Alliin lyase localization in bundle sheaths of the garlic clove (*Allium sativum*). *American Journal of Botany*, *81*, 89–94. https://doi.org/10.1002/j.1537-2197.1994.tb15413.x

Eratte, D., Wang, B., Dowling, K., Barrow, C. J., & Adhikari, B. P. (2014). Complex coacervation with whey protein isolate and gum arabic for the microencapsulation of omega-3 rich tuna oil. *Food and Function*, *5*(11), 2743–2750. https://doi.org/10.1039/c4fo00296b

Falsafi, S. R., Rostamabadi, H., Assadpour, E., & Jafari, S. M. (2020). Morphology and microstructural analysis of bioactive-loaded micro/nanocarriers via microscopy techniques; CLSM/SEM/TEM/AFM. *Advances in Colloid and Interface Science*, *280*, 102166. https://doi.org/10.1016/j.cis.2020.102166

Flanagan, S. E., Malanowski, A. J., Kizilay, E., Seeman, D., Dubin, P. L., Donato-Capel, L., Bovetto, L., & Schmitt, C. (2015). Complex equilibria, speciation, and heteroprotein coacervation of lactoferrin and β-lactoglobulin. *Langmuir*, *31*(5), 1776–1783. https://doi.org/10.1021/la504020e

Fukushima, S., Takada, N., Hori, T., Min, W., Wanibuchi, H., & Yamamoto, S. (2001). Suppression of chemical carcinogenesis by water-soluble organosulfur compounds 1. *The Journal of Nutrition*, *131*(3), 1049S–1053S. https://doi.org/10.1093/jn/131.3.1049S

García-Villalón, A. L., Amor, S., Monge, L., Fernández, N., Prodanov, M., Muñoz, M., Inarejos-García, A. M., & Granado, M. (2016). In vitro studies of an aged black garlic extract enriched in *S*-allylcysteine and polyphenols with cardioprotective effects. *Journal of Functional Foods*, *27*, 189–200. https://doi.org/10.1016/j.jff.2016.08.062

Gouin, S. (2004). Microencapsulation: Industrial appraisal of existing technologies and trends. *Trends in Food Science & Technology*, *15*, 330–347. https://doi.org/10.1016/j.tifs.2003.10.005

Grgić, J., Šelo, G., Planinić, M., Tišma, M., & Bucić-Kojić, A. (2020). Role of the encapsulation in bioavailability of phenolic compounds. *Antioxidants*, *9*(10), 923. https://doi.org/10.3390/antiox9100923

Huang, D., Ou, B., & Prior, R. L. (2005). The chemistry behind antioxidant capacity assays. *Journal of Agricultural and Food Chemistry*, *53*(6), 1841–1856. https://doi.org/10.1021/jf030723c

Huang, G., Shu, S., Cai, T., Liu, Y., & Xiao, F. (2012). Preparation and deproteinization of garlic polysaccharide. *International Journal of Food Sciences and Nutrition*, *63*(6), 739–741. https://doi.org/10.3109/09637486.2011.652599

Jaya, S., & Das, H. (2004). Effect of maltodextrin, glycerol monostearate and tricalcium phosphate on vacuum dried mango powder properties. *Journal of Food Engineering*, *63*(2), 125–134. https://doi.org/10.1016/S0260-8774(03)00135-3

17503841, 2023, 11, Downloaded from https://ift.onlinelibrary.wiley.com/doi/10.1111/1750-3841.16768 by Iskenderun Teknik Universitesi, Wiley Online Library on [15/01/2024]. See the Terms and Conditions (https://onlinelibrary.wiley.com/terms-and-conditions) on Wiley Online Library for rules of use; OA articles are governed by the applicable Creative Commons License

Jyothi, N. V. N., Prasanna, P. M., Sakarkar, S. N., Prabha, K. S., Ramaiah, P. S., & Srawan, G. Y (2010). Microencapsulation techniques, factors influencing encapsulation efficiency. *Journal of Microencapsulation*, *27*(3), 187–197. https://doi.org/10.3109/02652040903131301

Kelebek, H., Selli, S., Kadiroğlu, P., Kola, O., Kesen, S., Uçar, B., & Çetiner, B. (2017). Bioactive compounds and antioxidant potential in tomato pastes as affected by hot and cold break process. *Food Chemistry*, *220*, 31–41. https://doi.org/10.1016/j.foodchem.2016.09.190

Kim, J.-S., Kang, O.-J., & Gweon, O.-C. (2013). Comparison of phenolic acids and flavonoids in black garlic at different thermal processing steps. *Journal of Functional Foods*, *5*(1), 80–86. https://doi.org/10.1016/j.jff.2012.08.006

Kim, S., Kim, D.-B., Jin, W., Park, J., Yoon, W., Lee, Y., Kim, S., Lee, S., Kim, S., Lee, O.-H., Shin, D., & Yoo, M. (2017). Comparative studies of bioactive organosulphur compounds and antioxidant activities in garlic (*Allium sativum L.*), elephant garlic (*Allium ampeloprasum L.*) and onion (*Allium cepa L.*). *Natural Product Research*, *32*(10), 1193–1197. https://doi.org/10.1080/14786419.2017.1323211

Kuck, L. S., & Noreña, C. P. Z. (2016). Microencapsulation of grape (*Vitis labrusca* var. Bordo) skin phenolic extract using gum arabic, polydextrose, and partially hydrolyzed guar gum as encapsulating agents. *Food Chemistry*, *194*, 569–576. https://doi.org/10.1016/j.foodchem.2015.08.066

Kumari, A., Yadav, S. K., Pakade, Y. B., Singh, B., & Yadav, S. C. (2010). Development of biodegradable nanoparticles for delivery of quercetin. *Colloids and Surfaces B: Biointerfaces*, *80*(2), 184–192. https://doi.org/10.1016/j.colsurfb.2010.06.002

Lan, Y., Ohm, J.-B., Chen, B., & Rao, J. (2020). Phase behavior and complex coacervation of concentrated pea protein isolate-beet pectin solution. *Food Chemistry*, *307*, 125536. https://doi.org/10.1016/j.foodchem.2019.125536

Mendanha, D. V., Molina Ortiz, S. E., Favaro-Trindade, C. S., Mauri, A., Monterrey-Quintero, E. S., & Thomazini, M. (2009). Microencapsulation of casein hydrolysate by complex coacervation with SPI/pectin. *Food Research International*, *42*(8), 1099–1104. https://doi.org/10.1016/j.foodres.2009.05.007

Park, T., Oh, J.-H., Lee, J., Park, S. C., Jang, Y., & Lee, Y. (2017). Oral administration of (*S*)-allyl-L-cysteine and aged garlic extract to rats: Determination of metabolites and their pharmacokinetics. *Planta Medica*, *83*, 1351–1360. https://doi.org/10.1055/s0043-111895

Pinilla, C. M. B., Thys, R. C. S., & Brandelli, A. (2019). Antifungal properties of phosphatidylcholine-oleic acid liposomes encapsulating garlic against environmental fungal in wheat bread. *International Journal of Food Microbiology*, *293*, 72–78. https://doi.org/10.1016/j.ijfoodmicro.2019.01.006

Raghu, R., Lu, K.-H., & Sheen, L.-Y. (2012). Recent research progress on garlic (dà suàn) as a potential anticarcinogenic agent against major digestive cancers. *Journal of Traditional and Complementary Medicine*, *2*, 192–201. https://doi.org/10.1016/s2225-4110(16)30099-2

Rahman, M. S. (2009). Food stability beyond water activity and glass transition: Macro–micro region concept in the state diagram. *International Journal of Food Properties*, *12*(4), 726–740. https://doi.org/10.1080/10942910802628107

Rocha-Selmi, G. A., Bozza, F. T., Thomazini, M., Bolini, H. M. A., & Fávaro-Trindade, C. S. (2013). Microencapsulation of aspartame by double emulsion followed by complex coacervation to provide protection and prolong sweetness. *Food Chemistry*, *139*(1–4), 72–78. https://doi.org/10.1016/j.foodchem.2013.01.114

Rose, P., Whiteman, M., Moore, P. K., & Zhu, Y. Z. (2005). Bioactive *S*-alk(en)yl cysteine sulfoxide metabolites in the genus allium: The chemistry of potential therapeutic agents. *Natural Product Reports*, *22*(3), 351–368. https://doi.org/10.1039/b417639c

Sasmaz, H. K., Kadiroglu, P., Adal, E., Sevindik, O., Aksay, O., Erkin, O. C., Selli, S., & Kelebek, H. (2023). Optimization of black garlic production parameters using response surface methodology: Assessment and characterization of bioactive properties. *Journal of Applied Research on Medicinal and Aromatic Plants*, *34*, 100477. https://doi.org/10.1016/j.jarmap.2023.100477

Sasmaz, H. K., Sevindik, O., Kadiroglu, P., Adal, E., Erkin, Ö. C., Selli, S., & Kelebek, H. (2022). Comparative assessment of quality parameters and bioactive compounds of white and black garlic. *European Food Research and Technology*, *248*(9), 2393–2407. https://doi.org/10.1007/s00217-022-04055-2

Šeregelj, V., Ćetković, G., Čanadanović-Brunet, J., Tumbas Šaponjac, V., Vulić, J., & Stajčić, S. (2020). Encapsulation and degradation kinetics of bioactive compounds from sweet potato peel during storage. *Food Technology and Biotechnology*, *58*(3), 314–324. https://doi.org/10.17113/ftb.58.03.20.6557

Shahidi, F., & Han, X.-Q. (1993). Encapsulation of food ingredients. *Critical Reviews in Food Science and Nutrition*, *33*, 501–547. https://doi.org/10.1080/10408399309527645

Sharma, O. P., & Bhat, T. K. (2009). DPPH antioxidant assay revisited. *Food Chemistry*, *113*, 1202–1205. https://doi.org/10.1016/j.foodchem.2008.08.008

Speranza, B., Petruzzi, L., Bevilacqua, A., Gallo, M., Campaniello, D., Sinigaglia, M., & Corbo, M. R. (2017). Encapsulation of active compounds in fruit and vegetable juice processing: Current state and perspectives. *Journal of Food Science*, *82*(6), 1291–1301. https://doi.org/10.1111/1750-3841.13727

Tadros, T., Izquierdo, P., Esquena, J., & Solans, C. (2004). Formation and stability of nano-emulsions. *Advances in Colloid and Interface Science*, *108–109*, 303–318. https://doi.org/10.1016/j.cis.2003.10.023

Tavares, L., & Noreña, C. P. Z. (2020). Characterization of the physicochemical, structural and thermodynamic properties of encapsulated garlic extract in multilayer wall materials. *Powder Technology*, *378*, 388–399. https://doi.org/10.1016/j.powtec.2020.10.009

Tavares, L., Santos, L., & Noreña, C. P. Z. (2021). Microencapsulation of organosulfur compounds from garlic oil using β-cyclodextrin and complex of soy protein isolate and chitosan as wall materials: A comparative study. *Powder Technology*, *390*, 103–111. https://doi.org/10.1016/j.powtec.2021.05.080

Tavares, L., & Zapata Noreña, C. P. (2019). Encapsulation of garlic extract using complex coacervation with whey protein isolate and chitosan as wall materials followed by spray drying. *Food Hydrocolloids*, *89*, 360–369. https://doi.org/10.1016/j.foodhyd.2018.10.052

Tylkowski, B., Trojanowska, A., Giamberini, M., Tsibranska, I., Nowak, M., & Marciniak, Ł. (2017). Microencapsulation in food chemistry. *Journal of Membrane Science and Research*, *3*(4), 265–271. https://doi.org/10.22079/JMSR.2017.23652

Vera Candioti, L., De Zan, M. M., Cámara, M. S., & Goicoechea, H. C. (2014). Experimental design and multiple response optimization. Using the desirability function in analytical methods

17503841, 2023, 11, Downloaded from https://ift.onlinelibrary.wiley.com/doi/10.1111/1750-3841.16768 by Iskenderun Teknik Universitesi, Wiley Online Library on [15/01/2024]. See the Terms and Conditions (https://onlinelibrary.wiley.com/terms-and-conditions) on Wiley Online Library for rules of use; OA articles are governed by the applicable Creative Commons License

development. *Talanta*, *124*, 123–138. https://doi.org/10.1016/j.talanta.2014.01.034

Vidović, S. S., Vladić, J. Z., Vaštag, Žuž G., Zeković, Z. P., & Popović, L. M. (2014). Maltodextrin as a carrier of health benefit compounds in *Satureja montana* dry powder extract obtained by spray drying technique. *Powder Technology*, *258*, 209–215. https://doi.org/10.1016/j.powtec.2014.03.038

Yu, Y., & Lv, Y. (2019). Degradation kinetic of anthocyanins from rose (*Rosa rugosa*) as prepared by microencapsulation in freeze-drying and spray-drying. *International Journal of Food Properties*, *22*(1), 2009–2021. https://doi.org/10.1080/10942912.2019.1701011

Zhang, X., Li, N., Lu, X., Liu, P., & Qiao, X. (2014). Effects of temperature on the quality of black garlic. *Journal of the Science of Food and Agriculture*, *96*, 2366–2372. https://doi.org/10.1002/jsfa.7351

How to cite this article: Sasmaz, H. K., Adal, E., Kadiroğlu, P., Selli, S., Uzlasir, T., & Kelebek, H. (2023). Optimization of complex coacervation parameters for the production of encapsulated black garlic using response surface methodology. *Journal of Food Science*, *88,* 4424–4439. https://doi.org/10.1111/1750-3841.16768

17503841, 2023, 11, Downloaded from https://ift.onlinelibrary.wiley.com/doi/10.1111/1750-3841.16768 by Iskenderun Teknik Universitesi, Wiley Online Library on [15/01/2024]. See the Terms and Conditions (https://onlinelibrary.wiley.com/terms-and-conditions) on Wiley Online Library for rules of use; OA articles are governed by the applicable Creative Commons License